EN1
93105543

MODELLING OF NON-LINEAR RUBBER ISOLATORS

by
VISHWAS KHER

ME
1995
M
KHE
MOD

Th
ME/1995/m
K527m

DEPARTMENT OF MECHANICAL ENGINEERING
INDIAN INSTITUTE OF TECHNOLOGY KANPUR

MAY, 1995

MODELLING
OF
NON-LINEAR RUBBER ISOLATORS

A Thesis Submitted
in Partial Fulfillment of the Requirements
for the Degree of

Master of Technology

by

Vishwas Kher

to the

DEPARTMENT OF MECHANICAL ENGINEERING
INDIAN INSTITUTE OF TECHNOLOGY, KANPUR
May, 1995.

- 7 AUG 1996
CENTRAL LIBRARY
I. I. T., KANPUR
Acc. No. A. 122010

A122010

ME-1995-M-KHE-MOD

Certificate

This is to certify that the work contained in this thesis, entitled *Modelling of Nonlinear Rubber Isolators*, has been carried out by *Vishwas Kher* under our supervision and that this work has not been submitted elsewhere for a degree.

Dr. A. K. Mallik
Professor
Department of Mechanical Engineering
Indian Institute of Technology
Kanpur, INDIA

Dr. H. Hatwal
Professor
Department of Mechanical Engineering
Indian Institute of Technology
Kanpur, INDIA

May, 1995

POST GRADUATE OFFICE
I.I.T Kanpur.
Submitted on 5/5/95

ACKNOWLEDGEMENTS

I can, no way, articulate my grateful thanks to my guides and esteemed teachers Professor Mallik and Professor Hatwal for their excellent guidance, motivation and constant encouragement throughout the span of my thesis work. I am highly indebted to them for their magnanimous and benevolent attitude towards me, notwithstanding my numerous mistakes and at times considerable delay in carrying out the work. Their thoughtful way to approach a problem stressing upon the basic concepts has influenced and benefited me a lot.

I would like to gratefully acknowledge timely help from Mr. M. M. Singh. My sincere thanks are due to Mr. Vajpeyee for his help in signal digitization.

I express my deep appreciation and thanks to B. Ravindra, Rajiv Tiwari, Shyamal Chatarjee, Subbarao and Chandrashekhar who comforted me by their valuable suggestions and informative comments. I am indebted to my friend Sanjay Joshi for his obliging help in the electrical signal processing.

The sparkling and joyful company of all my friends gave me the vitality to continue with the work. In particular, I would like to mention Gujral, Mahesh, Nilesh, Rambhushan, Rao, Das and Shejul for coming to my rescue at a number of occasions.

Vishwas Kher

Abstract

Visco-elastic polymers like natural and synthetic rubbers (with various additives) are commonly used as vibration isolators. Such rubber elements provide both stiffness and damping as required by a good isolator. However, proper design can only be made only if their dynamic characteristics are correctly modelled.

In this thesis, a hollow cylindrical rubber specimen is tested under harmonic excitation for modelling its dynamic characteristics. A dynamic constitutive law, under harmonic loading, is proposed to fit the experimental results. Both the amplitude of deformation and frequency are varied in the range of interest for mechanical structural applications. Marked non-linearity is exhibited. The dependence of dynamic stiffness on the amplitude and a combination of linear hysteretic plus nonlinear Coulomb damping are seen to be essential for good modelling. For satisfactory modelling, future work should also take into account the effects of temperature.

Contents

1 Introduction **1**

1.1 Review of Previous Work 3

1.2 Present Work 4

2 Modelling of an Isolator through Harmonic Loading **6**

2.1 Modelling of an Isolator 7

2.2 Present Problem 12

3 Experimentation **16**

3.1 Set-up 16

3.2 Instrumentation 17

3.3 Signal Processing 20

4 Results and Discussion **24**

4.1 Static Stiffness 24

4.2 Natural Frequency 25

4.3 Frequency Dependence 27

4.4 Amplitude Dependence 30

4.5 Proposed Model 33

5 Conclusions **43**

5.1 Scope of future work 44

References **45**

Appendix **48**

List of Tables

4.1 Values of the constants in the constitutive equation 38

List of Figures

2.1 *Relationship between forcing function and response* 6

2.2 An isolator under vibrations (a) Base Excitation Case (b) External force excitation case 7

2.3 *Elastic restoring force* F_s vs. z 12

2.4 *Dissipative force* F_d vs. z 13

2.5 *Combined effect* $F(z, \dot{z})$ vs. z 14

2.6 *Freebody diagram of the isolator* 15

3.1 The rig 18

3.2 Instrumentation set-up 19

3.3 An example of filtering (base displacement signal of 0.15 mm amplitude at 120 Hz) 22

3.4 An example of phase-adjustment of the acceleration signal (Y-axis is acceleration or displacement; Scale not indicated) 23

4.1 Static stiffness curve 25

4.2 Natural frequency curve 26

4.3 Hysteresis loops (0.1 mm deformation amplitude; 50 Hz, 90 Hz and 150 Hz) 28

4.4 Damping Energy *vs.* Frequency (0.05 mm deformation amplitude) 29

4.5 Damping Energy *vs.* Frequency (0.1 mm deformation amplitude) 29

4.6 Damping energy *vs.* Relative amplitude (60 Hz, Solid line is the best fit line) 31

4.7 Damping energy *vs.* Relative amplitude (80 Hz, Solid line is the best fit line) 31

4.8 Hysteresis loops (0.05 mm, 0.1 mm, 0.15 mm, 0.25 mm, 0.3 mm deformation amplitude; 60 Hz) 32

4.9 Components of $F(z, \dot{z})$ 34

4.10 Variable Coulomb friction force employed in the model) 36

4.11 Experimental and simulated hysteresis loops (50 Hz, 0.1 mm deformation amplitude) 39

4.12 Experimental and simulated hysteresis loops (80 Hz, 0.25 mm deformation amplitude) 40

4.13 Experimental and simulated hysteresis loops (195 Hz, 0.1 mm deformation amplitude) 41

4.14 Experimental and simulated hysteresis loops (120 Hz, 0.15 mm deformation amplitude) 42

Chapter 1

Introduction

Resonance induced vibrations are detrimental in most of the engineering situations and may even lead to drastic failures. The sustenance of vibrations over long periods may cause sudden fatigue failure. The need for control of vibrations also arises in high precision measuring equipments. Frequently, one encounters the problem of protecting a machine or equipment from the vibrating foundation. On the other hand, the foundation may sometimes need to be protected from the vibrating machinery. An effective way of curbing the transfer of vibrations from the vibrating source is to have a resilient element with or without a damping element, known as an isolator. This method of vibration control is often used if it is not possible to eliminate the vibrations of the source.

Sometimes an isolator is designed to have both the resilience and damping. With remarkable upswing in the rubber technology, various synthetic rubbers and polymers have come up as promising materials for isolators as it is possible to combine both the properties in a single piece, unlike the structural materials where it is necessary to have separate dampers or inserts of high energy dissipation capacity materials since the damping capacity of structural materials is usually very small.

Rubber offers several other useful properties making it suitable to a large class of engi-

neering problems. It has extensive use in fatigue and noise control in industry *e.g.* drilling rods, grinders, circular saw blades. Light weight combined with above-mentioned qualities enhances its adoptability in the applications having weight reduction as a vital and uncomprisable objective such as aircraft industries or space applicatins. Its combination with structural materials is also in vogue.

Rubber and polymer properties undergo considerable change by variation of their constituents and hence desirable properties can be achieved. These properties are heavily dependent on temperature and frequency. To accommodate both temperature and frequency effects in a rubber or polymeric material, temperature effects are reduced to equivalent frequency with the help of master curves [1, 2] but even at a constant temperature several factors affecting the properties of these materials, namely, frequency, amplitude, time history, aging and type of excitation, demand attention from the designer. Application of rubber and polymers in a particular problem needs indentification of requirements of the problem and then judicious selection of material, shape, geometry and dimensions of isolaters, absorbers or any other vibration controlling element which needs prediction of the behaviour of these controlling elements in different sets of operating conditions [3, 4]. consequently, the need for the precise models for these materials accommodating aforesaid effects becomes manyfold.

Nevertheless, there has been greater motivation toward the study of rubber and polymeric materials in recent years which is reflected in the advances in the phenomenological theory of linear visco-elasticity and spectacular success in the synthesis of rubbers for attainment of stringent requirements imposed by specific problems.

The approach to the design changes for different applications. The modelling is concerned with obtaining a mathematical statement of the properties of the system, best expressed through a rheological constitutive equation, correlating the input and the response.

To avoid undue complications in the model, some simplifying assumptions are made and the system is idealized. Fixing the domain of the study is important from the view-point of pursuing solely the properties of interest. The analysis of the gross behaviour of the system is carried out by involving the basic unit properties of the component materials. The understanding of solid state or micromechanistic concepts for an engineer is also gaining significance, despite the fact that this approach has still not flourished to the point where it could become the sole basis of the complete design process. Ad-hoc testing can sometimes be taken up after analyzing the viability of the problem in terms of time, size and cost.

While specifically dealing with the modelling of rubber-like materials, its elastic properties should be studied with emphasis on the buckling behaviour. Hollow rubber specimens are vulnerable to buckling in compressive loading and generally have a low tensile strength. Abrasion resistance and other similar properties should also be given due attention if the application so requires. The damping in general is the most difficult to model. The temperature dependence of the elastic or loss modulus should be established, especially, if the transition region is near the room temperature.

1.1 Review of Previous Work

Recently, Tinker and Kutchins (1992) [5] investigated the damping phenomenon in wire rope isolators. They have reported that damping in typical wire rope isolator is predominately due to Coulomb friction. They developed a semi-empirical model involving n^{th} power damping and variable Coulomb friction damping. Harris and Stevenson (1986) [6] published the results for natural rubber (NR) and NR blends with high damping polymers. NR was found to be nearly linear in simple shear in both dynamic as well as static tests. Its behaviour was close to that of a steel spring but peak of the transimissiblity curve was low due to relatively high damping. Filled NR was drastically nonlinear and showed

dependence on frequency and amplitude of strain. As an extension to this work, Harris (1987) [7] investigated the effect of non-sinusidal input on rubber and noted that for complex vibrations consisting of many amplitudes and frequencies, the overall dynamic behaviour tends toward that obtained in single sine tests at a strain amplitude which corresponds to the largest amplitude that occurs in time history. Under a more and more complex system of vibration, nonlinear rubber shows greater linearity in behaviour and exhibits higher damping than indicated by their dynamic properties measured in conventional sinusoidal tests. Therefore, when the service enviornment of many components is taken into account, the dynamic behaviour of nonlinear rubber may give better performance characteristics than expected from conventional sine tests.

Medalia (1978) [8] discussed the effects of Carbon Black on dynamic properties of rubber vulcazinates and proposed empirical relations for loss modulous of rubber. In reference [9], elastic modulous and loss modulous of SBR (Styrene Buta-diene Rubber) containing particals of cross-linked polysterene have been obtained. Vinogradov and Pivovarov (1986) [10] introduced a hysteretic model comprising a linear viscous part and a nonlinear Davidenkov part in order to simulate rate and amplitude dependent internel losses. For a vibrating cable, parameter identification has been discussed and theoritical and experimental results have been compared. Iyenger (1979) [11] suggested an analytical model for the hysteretic behaviour of beams. The model was used to simulate several types of realistic softening hysteretic loops.

1.2 Present Work

This work is aimed at modelling a cylindrical rubber sleeve, commonly known as rubber spring, under harmonic loading. The rubber spring was used to isolate a known mass from a harmonically vibrating base plate. The objective was to obtain a constitutive equation

correlating the force with the instantaneous deformation and the instantaneous rate of deformation of the rubber isolator. For this, the base plate was sinusoidally excited using an electrodynamic shaker. The base displacement, top displacement and top acceleration signals were recorded and digitized. The deformation *i.e.* the relative displacement across the isolator and hysteresis loops were obtained by using the digitized displacement and acceleration data. The variation of area and shape of the hysteresis loops with frequency and amplitude was studied on the basis of which, a form of the damping was ascertained.

The frequency range under consideration was 20 Hz to 200 Hz which is also the range of interest in most of the industrial applications. The amplitude dependence of rubber properties has been established. The behaviour of the proposed model aggrees with experimental findings.

The thesis has been organised in the following way. The first section of Chapter 2 briefly discusses the general theory behind the modelling of an isolator and commonly prevelent methods thereof. The second part of the chapter defines the present problem and outlines the intended method of modelling. In Chapter 3, the description of the set-up and the instrumentation is given. The processing of the displacement and acceleration signals obtained through the experiments has been explained. Chapter 4 discusses the observations of the experiments and inferences drawn on the basis of them. The last section of this chapter analyses the inferences and establishes a mathematical model for the isolator. Chapter 5 concludes the thesis with a brief discussion about the scope of future work.

Chapter 2

Modelling of an Isolator through Harmonic Loading

A system undergoing mechanical vibrations has an input or forcing function and the response as its effect, as illustrated in Fig. 2.1. The relation between the forcing function and response depends on the properties of the system.

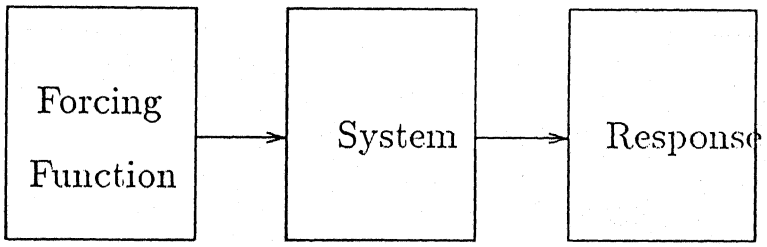

Figure 2.1: *Relationship between forcing functiion and response*

The modelling of the system defines the relationship between the input and the output in the form of a law or a constitutive equation. Thus, the modelling deals with the determination and the mathematical specification of the properties of the system from the input and response characteristics.

2.1 Modelling of an Isolator

The simplest type of a vibrating system is a single degree of freedom system in which the state of the system is completly determined by only one dependent variable. A single–degree–of–freedom system is modelled as a resilient member with or without energy dissipation mechanism connecting a mass and the foundation. An externel force acts on this system which sustains the vibrations. The resilient member is known to be an isolator when it is used to reduce the transfer of ill-effects of vibrations from the base to the mass (an equipment or machinery in practicl situations) or vice-versa. Two types of problems normally encountered in practice, for a harmonically excited single degree of freedom system, are shown in Fig. 2.2(a) and 2.2(b). In one class of the problems, the base on which

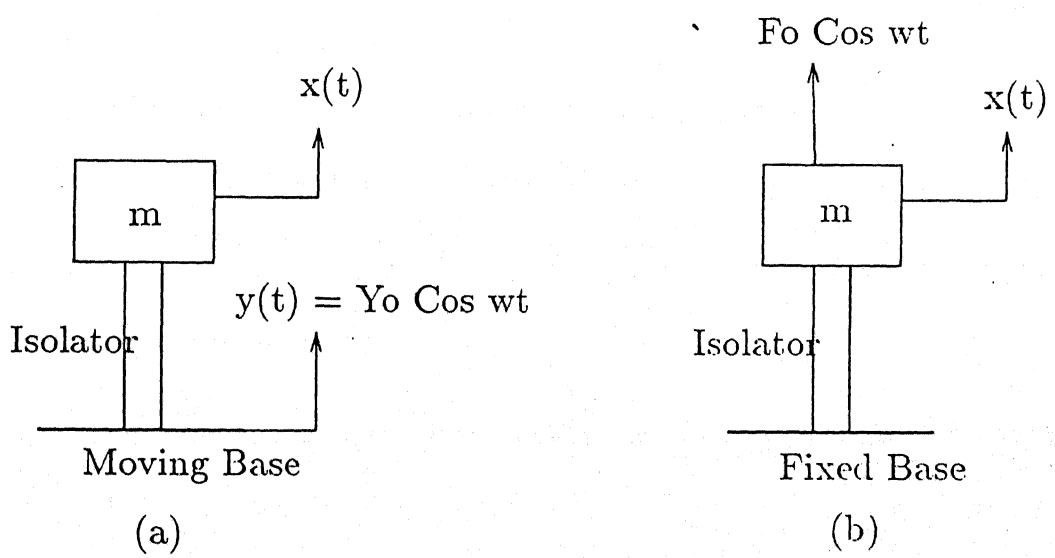

Figure 2.2: An isolator under vibrations (a) Base Excitation Case (b) External force excitation case

the system is mounted undergoes vibrations and causes the system to vibrate while in the

other, an externel force causes the vibrations of the system. Both of these problems in a linear system are mathematically equivalent.

A vibrating system may be subjected to several types of loading such as sinusoidal, saw-tooth wave force, a general periodic force or a random force. Out of these, sinusoidal loading is commonly encountered in the engineering practice as this is generally caused due to unbalance in rotating machineries which are widely used in the industry.

There are three properties of the system, *viz.* inertia, stiffness, and damping which govern the constitutive equation of a vibrating system. The general form of constitutive equation for a harmonically excited single degree of freedom system is written as

$$m\ddot{x} + F(x, \dot{x}) = F_0 cos\omega t \tag{2.1}$$

In the base excitation case [Fig. 2(a)], it can be alternatively written as

$$m\ddot{x} + F(z, \dot{z}) = 0 \tag{2.2}$$

where $z = x - y$ is the relative displacement of the mass with respect to the base and $\dot{z} = \dot{x} - \dot{y}$ is the relative velocity. The $F(z, \dot{z})$ term involves

(i) Restoring force $F_s(z)$ which depends on the stiffness of the system. This is a function of the deformation of the isolator, z and does not involve $\dot{z}$.

(ii) Damping force term $F_d(z, \dot{z})$ which is responsible for the energy dissipation of the system. This is rate dependent and may involve both z and $\dot{z}$. Therefore, $F(z, \dot{z})$ is written as

$$F(z, \dot{z}) = F_d(z, \dot{z}) + F_s(z) \tag{2.3}$$

Equations 2.1 and 2.2 may, in general, take the form of a nonlinear differential equation. This nonlinearity depends on a number of factors. In particular, material of the isolator plays an important role. For example, in rubbers and polymers the stiffness is

found to be nonlinear. These materials do not follow Hooke's law and may show hardening or softening characteristics with increasing strain. Structural materials have linear stiffness in the elastic range but may considerably deviate from linearity in the plastic range. The dynamic properties of rubbers and polymers have been observed to be heavily dependent on the frequency. The stiffness of these materials may undergo large change depending on the frequency. It may or may not depend on the stress amplitude. Similarly, the damping which is a measure of energy dissipation capacity, may also depend on the frequency and amplitude of vibration. If either damping or stiffness depends on the vibration amplitude, the material shows nonlinear behaviour.

Based on the above-mentioned characteristics, damping may be of three types.

(a) Rate independent or frequency independent which is also called the hysteretic damping.

(b) Linear dashpot damping or viscous damping in which the damping force increases linearly with frequency.

(c) General frequency dependent damping which is observed in many anelastic and visco-elastic materials. In this, the damping energy is a function of frequency. Case(b) is only a special case of this.

In linear damping, the energy dissipation is proportional to the square of the amplitude. Various synthetic rubbers, polymers and rubber-like materials exhibit the third type of damping. For these materials, the force–deformation relationship is rate-dependent. They are modelled by a combination of viscous and elastic elements in order to represent both damping and stiffness. In the most general case, the force–

deformation relationship in a visco-elastic material is expressed as

$$\left[a_0 + a_1\left(\frac{\partial}{\partial t}\right) + a_2\left(\frac{\partial^2}{\partial t^2}\right) + \cdots\right]\sigma = \left[b_0 + b_1\left(\frac{\partial}{\partial t}\right) + b_2\left(\frac{\partial^2}{\partial t^2}\right) + \cdots\right]\epsilon \qquad (2.4)$$

For harmonic excitation $\sigma = \sigma_0 e^{j\omega t}$ and $\epsilon = \epsilon_0 e^{j\omega t}$, this reduces the above equation to

$$\left[a_0 + a_1(j\omega) + a_2(j\omega)^2 + ...\right]\sigma_0 = \left[b_0 + b_1(j\omega) + b_2(j\omega)^2 + ...\right]\epsilon_0 \qquad (2.5)$$

or

$$E^* = \frac{\sigma_0}{\epsilon_0} = \frac{[B_1(\omega) + jB_2(\omega)]}{[A_1(\omega) + jA_2(\omega)]} \qquad (2.6)$$

or

$$E^* = E'(\omega) + jE''(\omega) \qquad (2.7)$$

This can be alternatively expressed as $F = K^* x$ or

$$F = (K'(\omega) + jK''(\omega))\, x \qquad (2.8)$$

K^* is known as the complex stiffness, $K'(\omega)$ is known as the storage modulus and associates force F in phase with the displacement x. $K''(\omega)$ is known as the loss modulus and associates the force 90° out of phase with the displacement x. The visco-elastic properties show remarkable dependence on the temperature also, so K' and K'' may be functions of temperature as well.

The major shortcoming of the above model with a's and b's as constants is that they cannot accomodate stress and strain dependent behaviour observed in several nonlinear materials. The properties of some of these nonlinear materials are affected by the stress-history, temperature, static mean stress, frequency or the amplitude of the stress.

If $F(z, \dot{z})$ is plotted against z [refer equation 2.2], the curve obtained is a loop which is called hysteresis loop. The shape and area enclosed by the loop can reveal

much about the above-mentioned characteristics and consequently, are of paramount importance in the modelling of nonlinear materials. The area of the loop gives the energy dissipated per cycle. The damping energy per cycle can be expressed as

$$D = \oint F_d(z, \dot{z}) dz \tag{2.9}$$

The linear damping exhibits elliptical hysteresis loops whose area is propertional to the square of the deformation amplitude. In other words the damping energy is expressed as $E_{damp} \propto Z^n$ with $n = 2$ and Z is the amplitude. In some polymers and elastomers, n is greater than 2, but the shape of the loop remains close to elliptical. In others, not only is n greater than 2, but the shape of the loop is very different from elliptical.

One imporatant class of nonlinear damping is Coulomb Friction damping in which the damping force is independent of the magnitude of the velocity. For this type of damping, the energy disssipation is proportional to the amplitude *i.e.* $n = 1$. The hysteresis loop obtained is a parallelogram if the stiffness is linear.

The inclination of the hysteresis loop indicates the stiffness of the system and is governed by $F_s(z)$ [refer eqn. 2.3] whereas the area of the loop is governed by $F_d(z, \dot{z})$. Figures 2.3, 2.4 and 2.5 explain how the hysteresis loop in Fig. 2.5 is obtained by superimposing $F_s(z)$ *vs.* z curve in Fig. 2.3 and $F_d(z, \dot{z})$ *vs.* z, shown in Fig. 2.4.

Besides energy dissipation per cycle *i.e.* the area of the hysteresis loop, other measures of damping capacity are sometimes used. Some of them are less common and are applicable to special class of problems only. Some of these measures are logrithmic decreement, half-power band width and resonance magnification factor. The loss

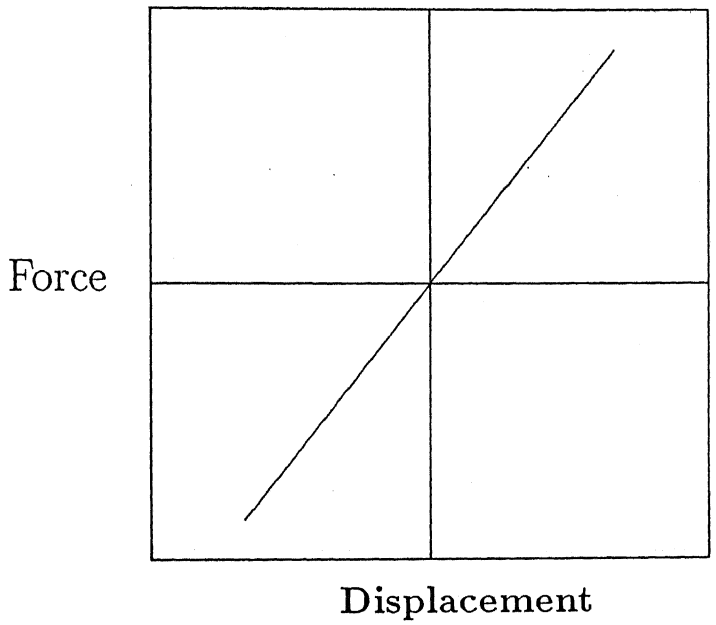

Figure 2.3: *Elastic restoring force* F_s vs. z

factor is a widely used measure of damping. It is defined as

$$\eta = \frac{D}{2\pi U} \tag{2.10}$$

where D is the damping energy per cycle and U is the maximum strain energy stored in the system during the cycle. The dependence of damping energy, stiffness and other properties on frequency, temperature, amplitude, mean static stress etc. is required to be considered for the modelling problem.

2.2 Present Problem

The objective is to model a rubber isolator. The isolator was made of natural rubber with Carbon Black fillers. The rubber isolater was mounted on an electrodynamic shaker and was fixed with a mass at the top. The base, on which the isolator was mounted, was harmonically excited. The sinusoidal excitation was selected for the

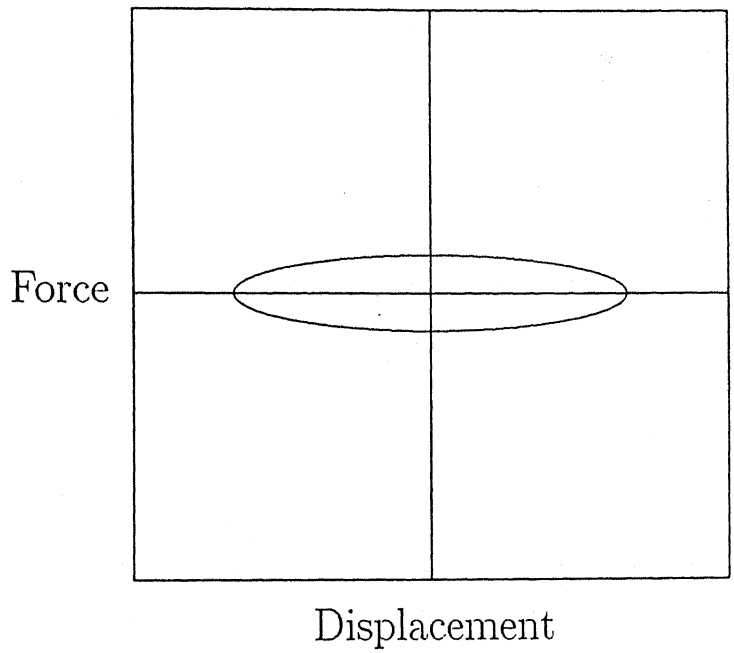

Figure 2.4: *Dissipative force* F_d vs. z

experiments because sinusoidal loading is encountered in a number of engeering problems. Secondly, non-sinusoidal periodic loading can be represented as the summation of its Fourier components and thus can be analyzed through superposition of the effects of individual sine components. Therefore, this system can be modelled as a single degree of freedom system harmonically excited at the base. The freebody diagram of the system is shown in Fig. 2.6. The rubber isolator is attached to the moving base and the force acting on the rubber isolator is expressed as a function of the relative displacement and the relative velocity of the mass with respect to the base *i.e.* as a function of the deformation and rate of deformation of the rubber spring. The constitutive equation from equation 2.2 can be written as

$$m\ddot{x} + F(z, \dot{z}) = 0$$

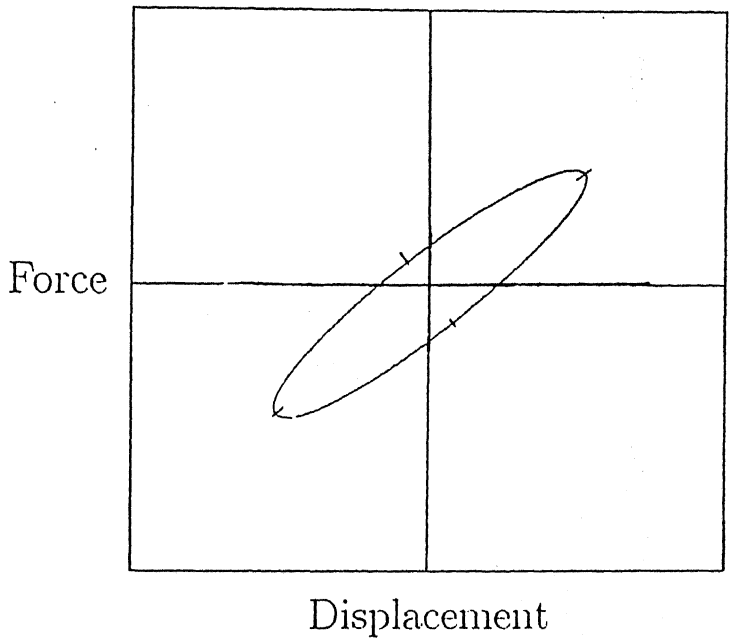

Figure 2.5: *Combined effect* $F(z, \dot{z})$ vs. z

In order to determine the exact form of $F(z, \dot{z})$, acceleration $\ddot{x}$ of the mass and deformation z across the isolator are needed. Two pick-ups, one at the base and the other at the top, were used for obtaining $\ddot{x}$, x and y. The hysteresis loop is obtained by plotting $F(z, \dot{z})$ against z, where $F(z, \dot{z})$ is given by $-m\ddot{x}$. The area of the hysteresis loop was used as a measure of the damping capacity. experiments were conducted for studying (i) the damping energy with frequency behaviour keeping base displacements such that the relative displacement across the isolator *i.e.* the deformation, is constant (ii) the damping energy with deformation of the isolator at constant frequencies.

Although rubbers and polymers may have large dependence on the temperature, the temperature dependence was not undertaken for the study and the experimentas were conducted at room temperature. Similarly, the stress-history effect was also not investigated.

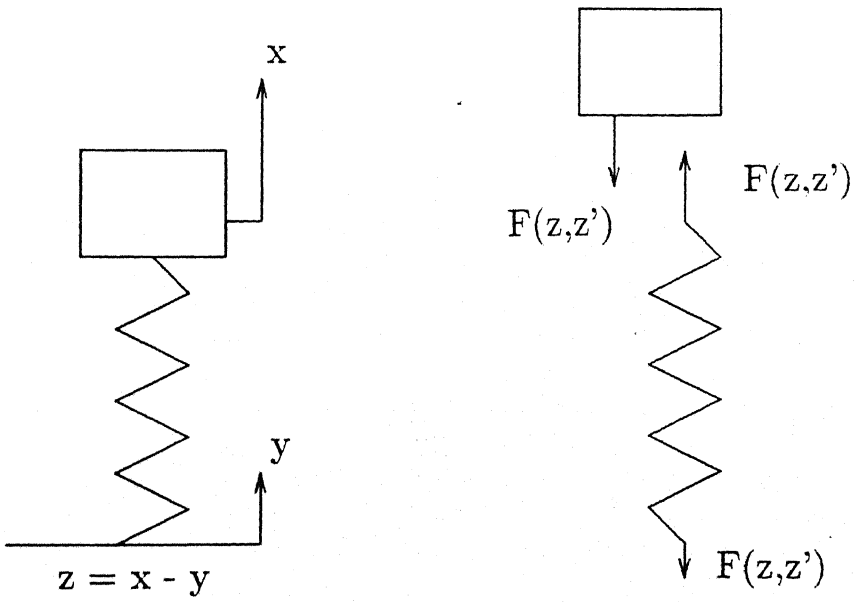

Figure 2.6: *Freebody diagram of the isolator*

Chapter 3

Experimentation

3.1 Set-up

A cylindrical sleeve made of Natural Rubber with Carbon Black fillers (IRHD 40) was used as the isolator. The external and internal diameters of the rubber spring were 34.8 mm and 21.2 mm respectively and the height was 98.1 mm. The sketch of the rig is shown in Fig. 3.1. The rubber cylinder at one end was attached to a cast iron plate (2) through hose clamp and adhesive. The rubber sleeve–cast iron plate assembly was fixed in a housing (3) serving as the support for the rubber sleeve and the top plate. The projected ends of the base of the housing have two open U-slots. A base plate (5) was constructed for facilitating the mounting of this assembly on an electrodynamic shaker. The base plate has seven countersunk through-holes for fixing it at the top of the shaker. The housing containing the rubber sleeve was mounted on the base plate by fastening two bolts (not shown in the figure) through U-slots of the housing and two additional holes in the base plate. In order to increase the mass at the top of the rubber cylinder, a mild steel block (1) was screwed to the top of the plate (2).

3.2 Instrumentation

As discussed in Chapter 2, acceleration $\ddot{x}$ of the mass and the deformation z of the rubber spring are needed for obtaining the hysteresis loops. For this, three signals *viz.* acceleration and displacement at the top and the displacement at the base, were recorded. Two B & K 4370 accelerometers, one at the top plate and ther other at the base plate, were used to pick up the acceleration signals as shown in Fig. 3.2. These signals were amplified by using two B & K 2635 charge amplifiers and integrated twice to give the displacement signals. The deformation of the isolator was obtained by taking the difference of the displacement signals at the top and the base. Since the phase of the signal may undergo some shift in the amplification and integration process, it was ensured that both the amplifiers were always at the same settings which would reduce the possibility of unequal phase phase shift in the two signals, because any error in the relative phase of the two signals could lead to erroneous results. The lower and higher cut-off frequenies were 1 Hz and 3 KHz in the displacement mode and 2 Hz and 3 KHz in the acceleration mode. The amplification in the displacement mode was 1000 mV/unit out till 120 Hz and 100 mV/unit out at higher frequencies. The amplification in the acceleration mode was 10 mV/unit out for the entire frequency range.

The signals were observed on Kikusui COR 5501U Two Channel Digital Storage Oscilloscope. The oscilloscope had a 4 kilobyte memory for each channel, so the signals could be stored simultaneously. The signals were digitized and transferred to a microcomputer through RS232C. A waveform on the CRT screen of the oscilloscope had 4096 *(horizontal)* $\times$ 256 *(vertical)* resolution. Therefore, a digitized signal could have 4096 data points out of which 4000 points were recorded.

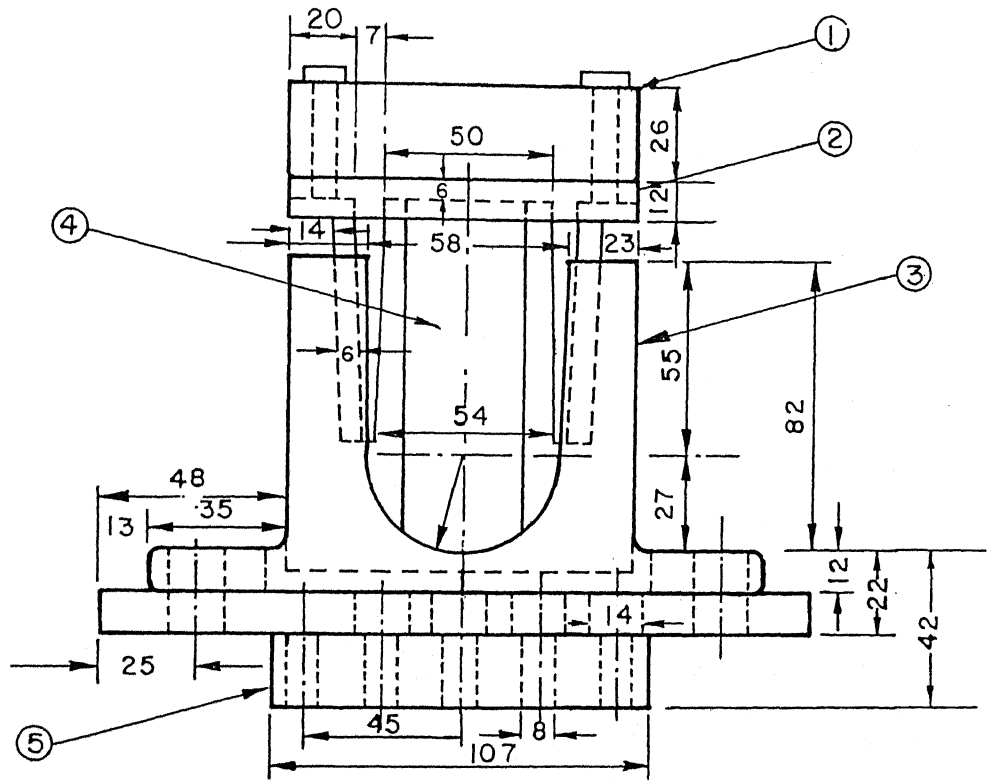

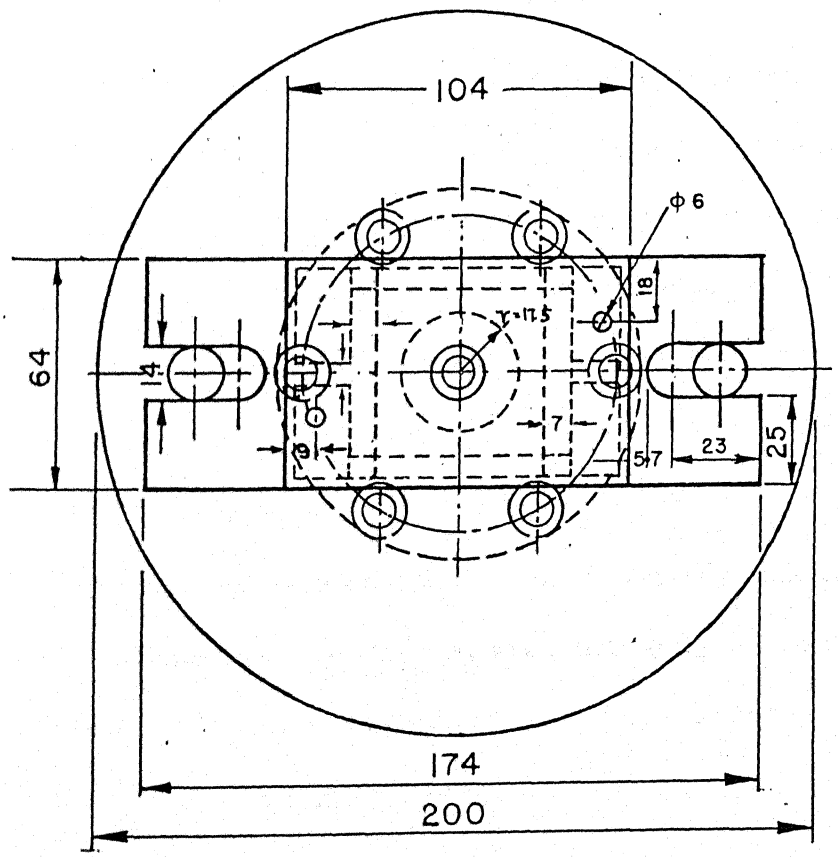

1. Steel block (M.S)
2. Top plate (C.I)
3. Housing (C.I)
4. Rubber spring (Natural rubber)
5. Base plate

Figure 3.1: The rig

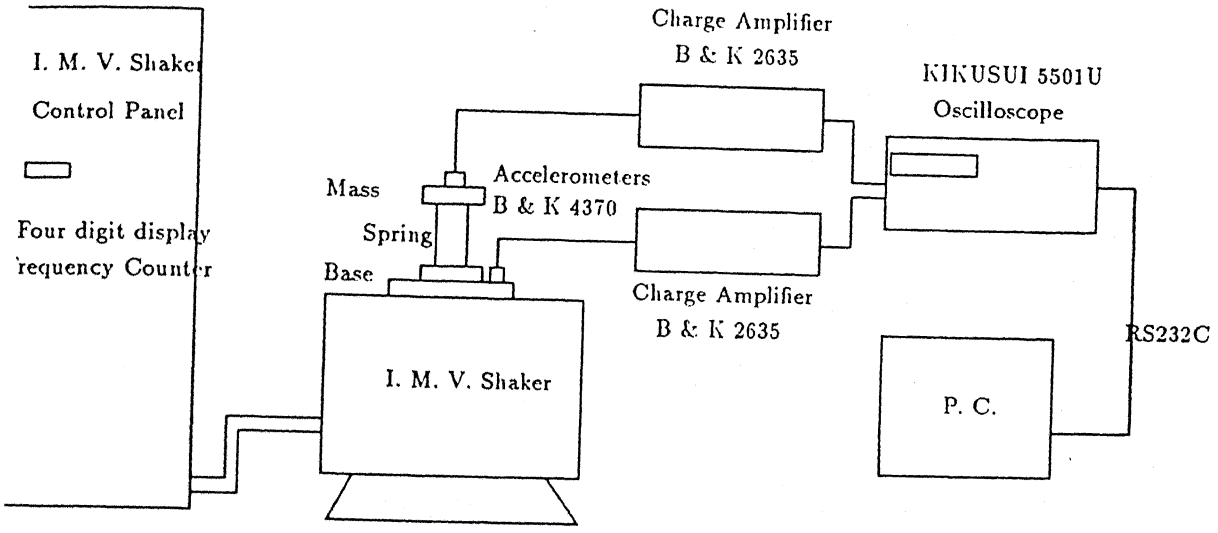

Figure 3.2: Instrumentation set-up

The acceleration of the top plate was also to be recorded along with the displacements at the top and the base. However, since the oscilloscope had only 2 channels, all the signals could not be recorded simultaneously. The two displacements signals were recorded separately. But this caused the incompatibility in the phase of the acceleration signal and the two displacement signals as they were recorded at different time instants. The incompatibility of the phase was corrected later during the signal processing which is discussed in the next section.

The base plate was excited by I. M. V. electrodynamic shaker having pneumatic suspension base. The frequency was monitored by the digital display on the control panel of the shaker and cross-checked with the oscilloscope using vertical cursors on the CRT screen of the oscilloscope.

The damping energy variations (i) with frequency (from 20 Hz to 200 Hz in steps

of 20 Hz) at a constant deformation amplitude of the rubber spring, and (ii) with deformation amplitude (0.05 mm to 0.3 mm at every 0.05 mm) at a constant frequency, were studied. In the first set of experiments, three values of the deformation amplitude, namely, 0.05 mm, 0.1 mm and 0.15 mm, were used to study the damping energy with frequency behaviour. In the latter catagory, three representative frequencies, viz. 60 Hz, 80 Hz and 120 Hz were used. The amplitude of the deformation was monitored on the oscilloscope using subtraction mode of the oscilloscope which gives the difference of the signals being supplied to the two channels.

A list of specifications of the equipments used is given in the appendix-A.

3.3 Signal Processing

After digitizing the three signals, the high frequency noise was filtered out using linear phase-shift, causing equal phase shift in all the signals, low pass filter. The cut-off frequency used was 3 kHz. A signal before and after filtering is shown in Fig. 3.3.

It has been discussed in Chapter 2 that the hysteresis loop is obtained by plotting $F(z, \dot{z})$ against deformation z. $F(z, \dot{z})$ equals $-m\ddot{x}$ which means that it is 180° out of phase with the acceleration $\ddot{x}$ of the mass at the top. Acceleration $\ddot{x}$ in turn is 180° out of phase with the displacement x of the top, thus the force $F(z, \dot{z})$ and the displacement x are in the same phase. Therefore, the recorded acceleration signal was processed to have the same phase as that of the displacement signal of the top plate and multiplied by mass m, so as to give a measure of the force $F(z, \dot{z})$. Since the acceleration signal at the top was not measured simultaneously with the displacement signals, the initial phase of the acceleration signal (Fig. 3.4) is synchronized with that of the displacement signal.

After this, the deformation of the rubber was obtained by subtracting the base displacement from the top displacement. $F(z, \dot{z})$ obtained from the recorded acceleration by the above procedure was plotted against z to get the hysteresis loop. Its area was calculated numerically using trapezoidal rule on the data points recorded in the PC.

CENTRAL LIBRARY
I. I. T., KANPUR
Acc. No. A.122010

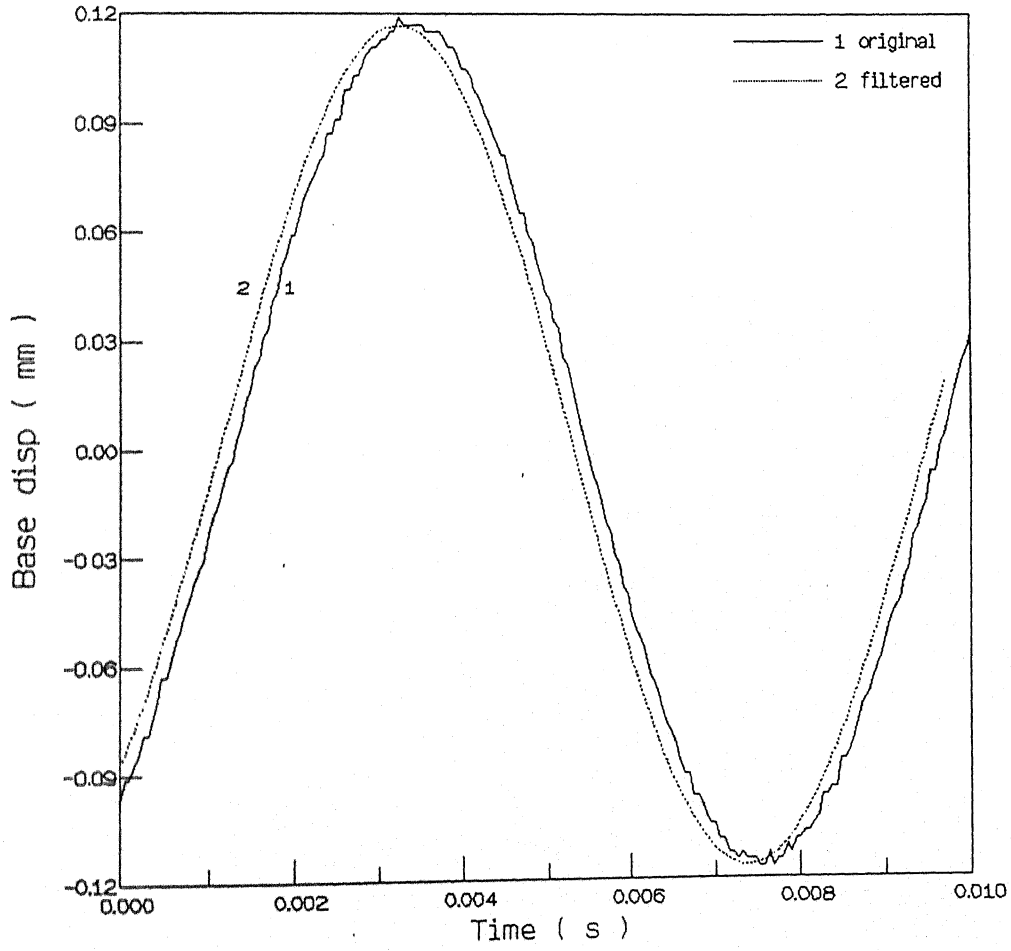

Figure 3.3: An example of filtering (base displacement signal of 0.15 mm amplitude at 120 Hz)

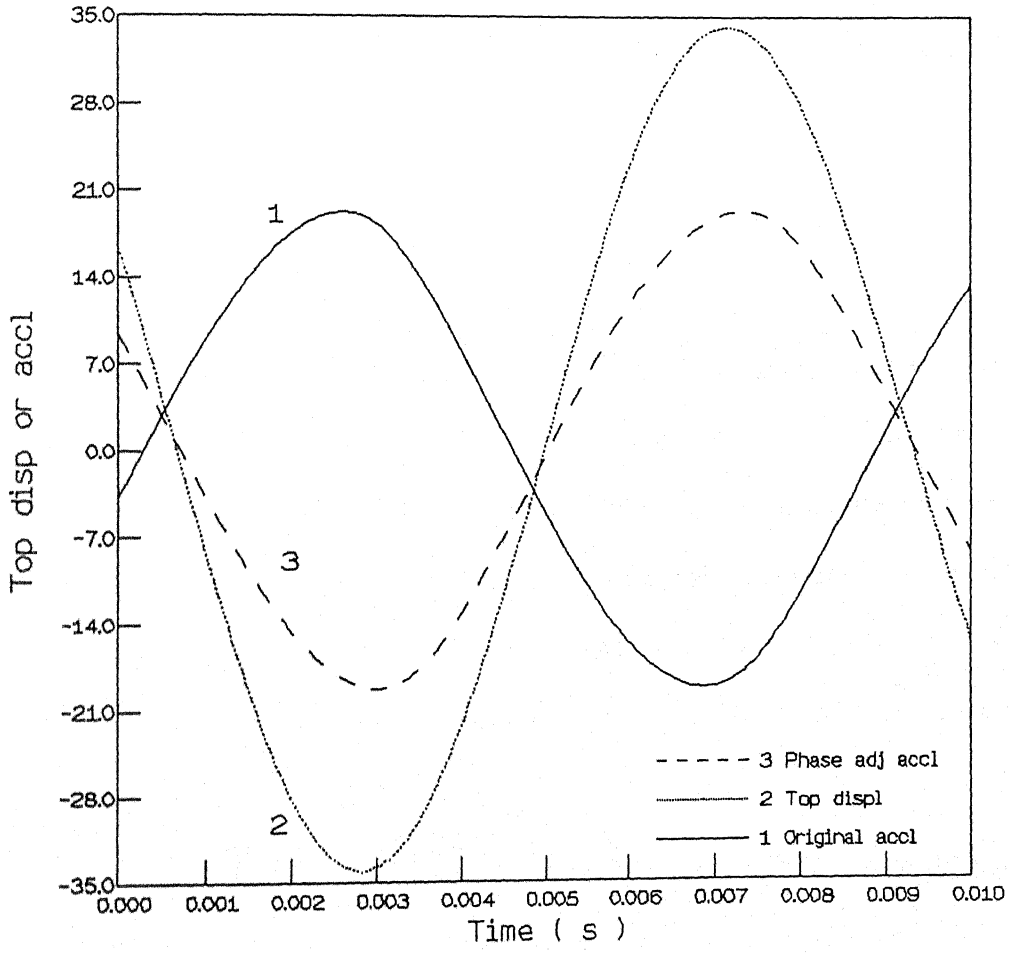

Figure 3.4: An example of phase-adjustment of the acceleration signal (Y-axis is acceleration or displacement; Scale not indicated)

Chapter 4

Results and Discussion

4.1 Static Stiffness

As discussed in chapter 2, the modelling of the system requires the determination of the term $F(z, \dot{z})$ which consists of the damping term $F_d(z, \dot{z})$ and the stiffness term $F_s(z)$. The stiffness is one of the three properties of the system governing its behaviour in vibrations. In a large class of rubber-like materials, the stiffness of the material in dynamic testing may show marked departure from the static stiffness. yet, static stiffness gives an overall idea of the nature of the force–deformation relationship of the material.

The static stiffness test in compression was conducted on Universal Testing Machine INSTRON 1195. The maximum comprtession was limited to 0.5 mm since in the dynamic test, the maximun deformation amplitude was 0.3 mm. It should be emphasized that the static stiffness experiment could not be done accurately because the sidewise deformation of the rubber spring could not be entirely eliminated. This resulted in some eccentricity of the loading, which violated the condition of uniaxial stress in the static stiffness test in compression. The experimental static stiffness curve is shown

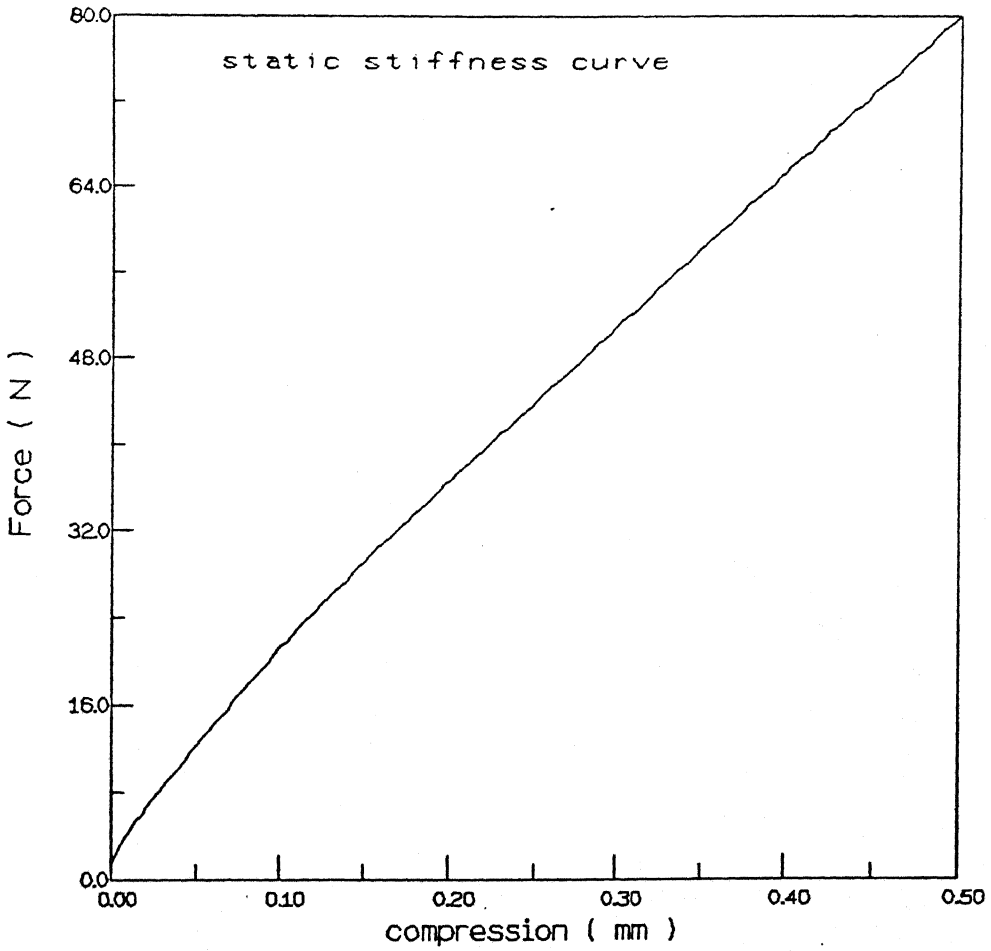

Figure 4.1: Static stiffness curve

in Fig. 4.1. It is observed that the rubber spring is softening type.

4.2 Natural Frequency

The natural frequency of this system can be quite accurately determined by determining the frequency at which the relative transmissibility of the system reaches the maximum value for a constant value of the base displacement amplitude. The spring-mass system was excited with a constant base amplitude of 0.1 mm and the relative

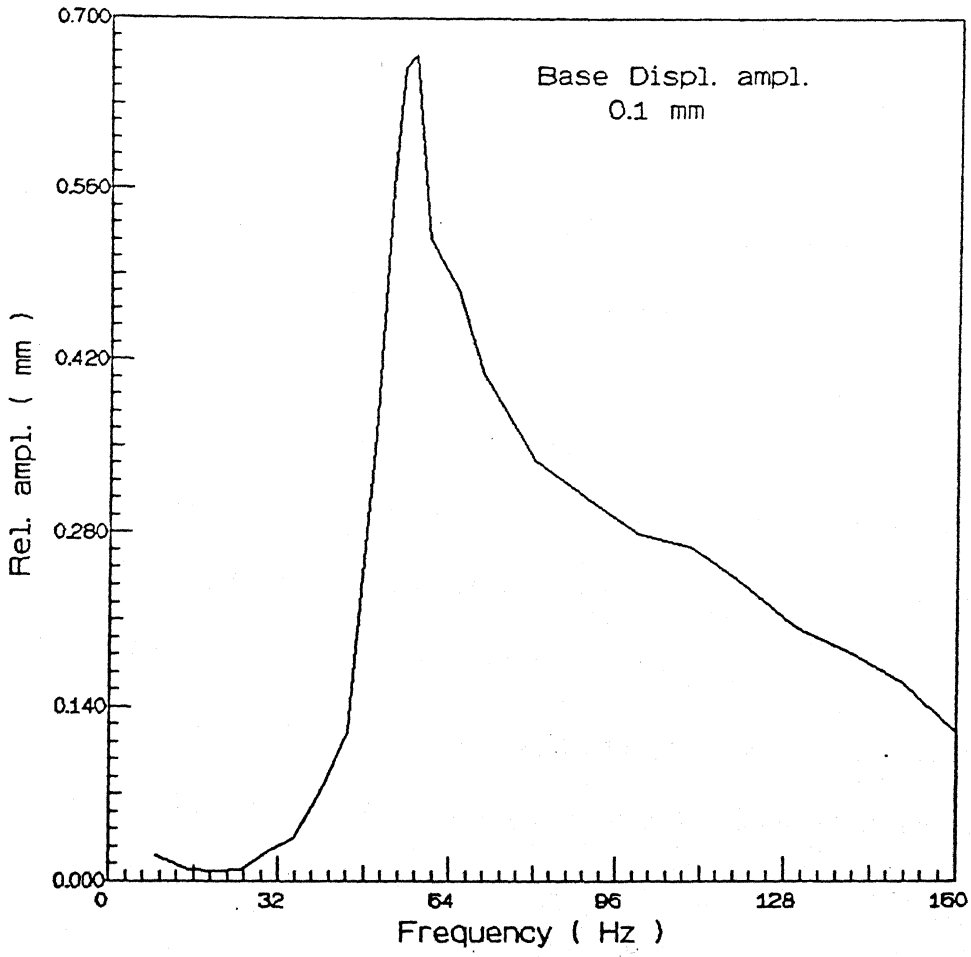

Figure 4.2: Natural frequency curve

amplitude of the mass *i.e.* the deformation amplitude across the rubber spring was measured at different frequencies. The deformation amplitude is plotted against the frequency in Fig. 4.2. It is observed that this response curve is typical of the Voigt model. The natural frequency from Fig. 4.2 is observed to be 57 Hz.

4.3 Frequency Dependence

The frequency dependence of the stiffness of the rubber spring material is best observed through the hysteresis loops. Fig. 4.3 shows three hysteresis loops obtained through the procedure described in section 2.2 and 3.3. The loops 1, 2 and 3 are at constant frequencies 50 Hz, 90 Hz and 150 Hz with the base excitation being set up to such amplitude that the maximum relative displacement across the rubber spring *i.e.* the deformation of the rubber spring in each case is obtained as 0.1 mm. These hysteresis loops resemble ellipses but are pointed at the ends. Largely elliptical shape of the loops indicates the dominance of the viscous or n^{th} power damping. The inclination of the loop which is governed by the stiffness of the system remains nearly unchanged with frequency. The constant inclination of the hysteresis loops was observed at other values of the deformation amplitudes also.

The area of the hysteresis loops gives the damping energy of the specimen per cycle. The damping energy variation with frequency at constant deformation amplitude are plotted in figures 4.4 and 4.5 for 0.05 mm and 0.1 mm deformation amplitude, respectively. It is seen

that there is no clear trend in the behaviour of the damping energy variation with frequency. However, the scatter in Figs. 4.4 and 4.5 can be seen to be about a mean value of constant energy dissipation. Therefore, in the absence of a clearcut trend in Figs. 4.4 and 4.5, it is reasonable to assume that the energy dissipation is independent of frequency in the small range of the frequency considered in this work.

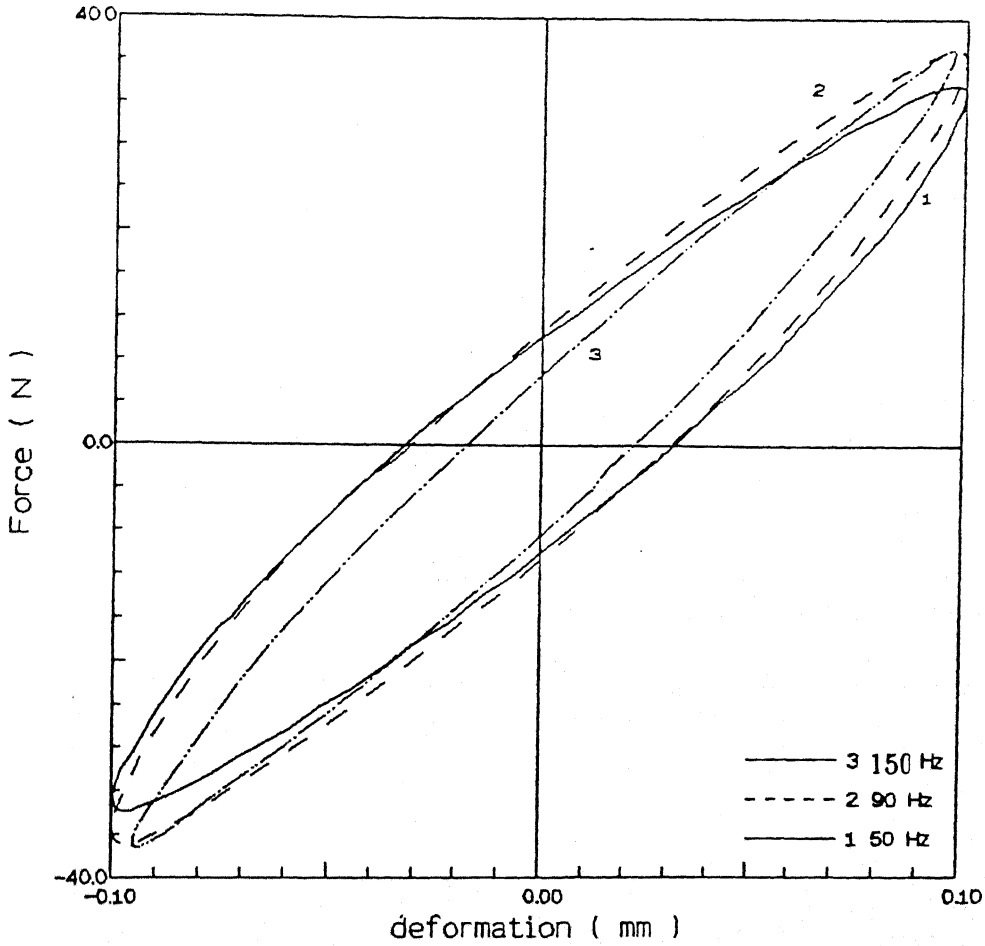

Figure 4.3: Hysteresis loops (0.1 mm deformation amplitude; 50 Hz, 90 Hz and 150 Hz)

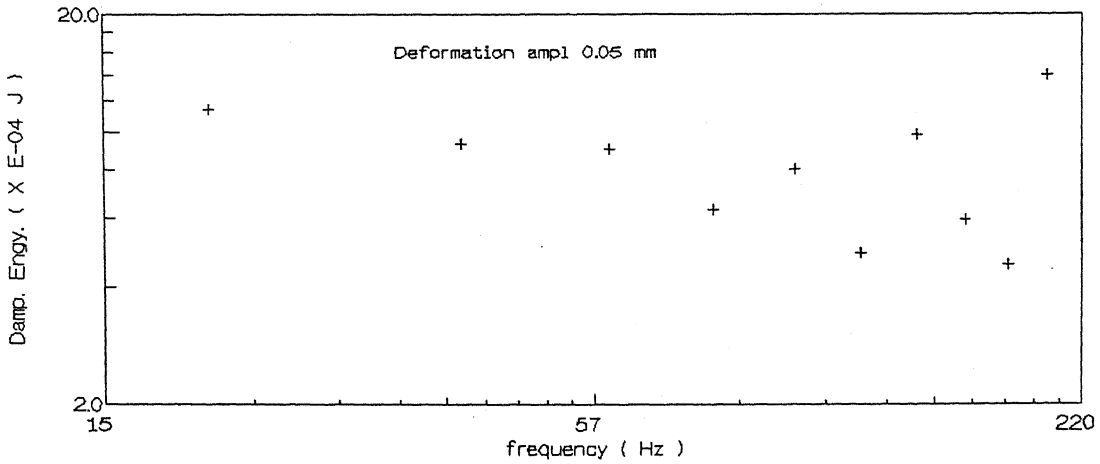

Figure 4.4: Damping Energy *vs.* Frequency (0.05 mm deformation amplitude)

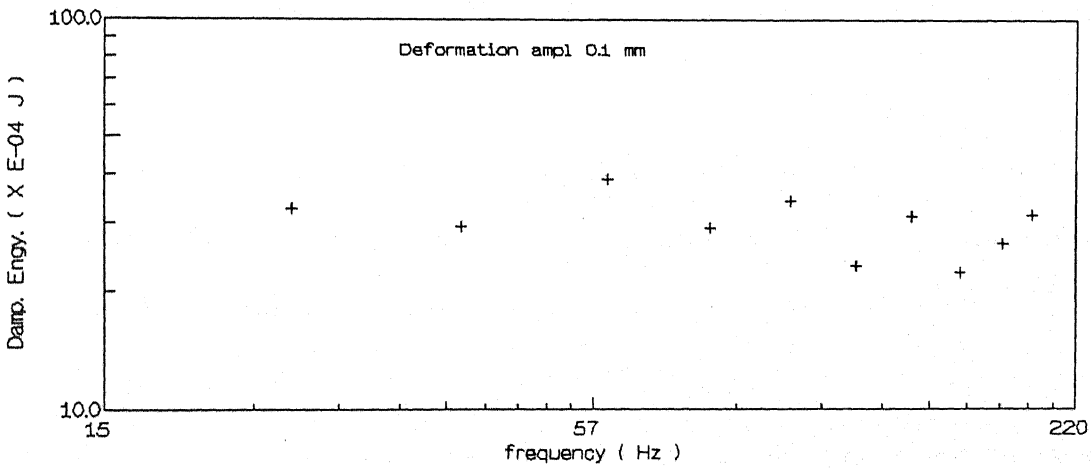

Figure 4.5: Damping Energy *vs.* Frequency (0.1 mm deformation amplitude)

4.4 Amplitude Dependence

In order to study the amplitude dependence of the system, experiments were conducted for six different values of deformation amplitude of the rubber spring ranging from 0.05 mm to 0.3 mm in steps of 0.05 mm, keeping the frequency constant. The energy dissipated per cycle is plotted against the deformation amplitude for 60 Hz and 80 Hz in figures 4.6 and 4.7, respectively.

The solid line in the figure is best fit line. The slope of this line is p assuming $E_{damp} \propto |Z_0|^p$ where $|Z_0|$ is the deformation amplitude. It can be seen that at both the frequencies, the damping energy variation with amplitude has an index, p, less than 2 which can be calculated by $\frac{\triangle \ln E_{damp}}{\triangle \ln Z_0}$. The departure of p from 2 implies that this system cannot have the full contribution of linear viscous or hysteretic damping which have an index of 2, as discussed in Chapter 2. In n^{th} power damping, the damping force is given by $F_d = (|\dot{x}|^n sgn(\dot{x}))$. This gives the damping energy $E_{damp} \propto |X|^{n+1}$. Thus with p less than 2 for the rubber spring, as observed above, the index n should be less than 1.

Figure 4.8 shows the hysteresis loops at 60 Hz for five different values of the deformation amplitude. An important observation from Fig. 4.8 is that the inclination of the loop decreases with increasing deformation amplitude. The dynamic stiffness curve [12,13] or the backbone curve is the curve obtained by joining the midpoints of those points on the upper and lower branches of the hyseresis loop that have same values of the displacement.

Figure 4.8 exhibits that all the hysteresis loops closely resemble ellipses. This indicates that the backbone curves are straight lines along the major axes. Similar tests were conducted at 80 Hz and 120 Hz and again the shape of the hysteresis loops was

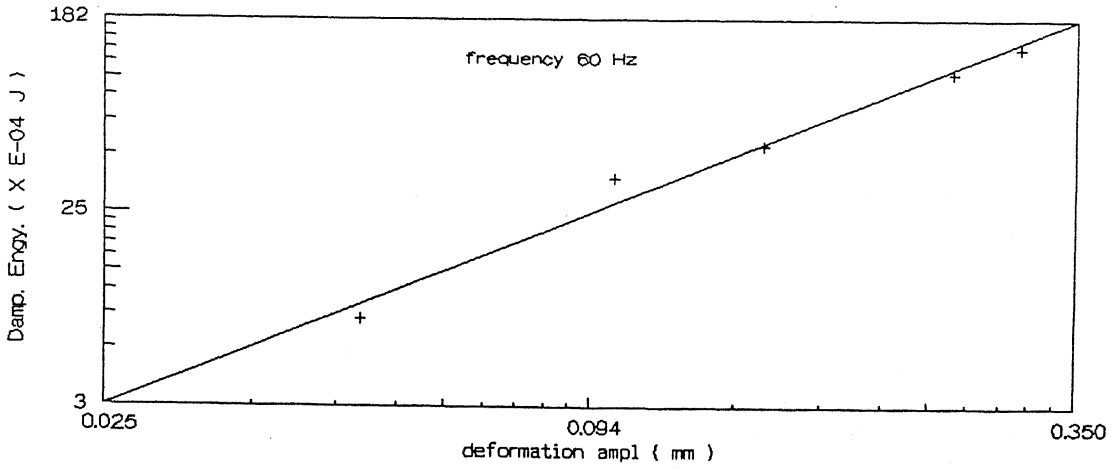

Figure 4.6: Damping energy *vs.* Relative amplitude (60 Hz, Solid line is the best fit line)

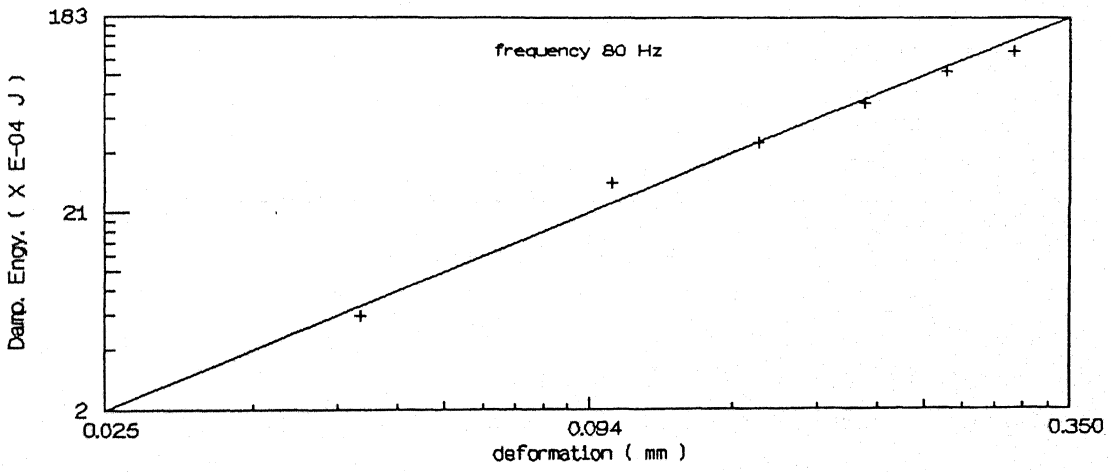

Figure 4.7: Damping energy *vs.* Relative amplitude (80 Hz, Solid line is the best fit line)

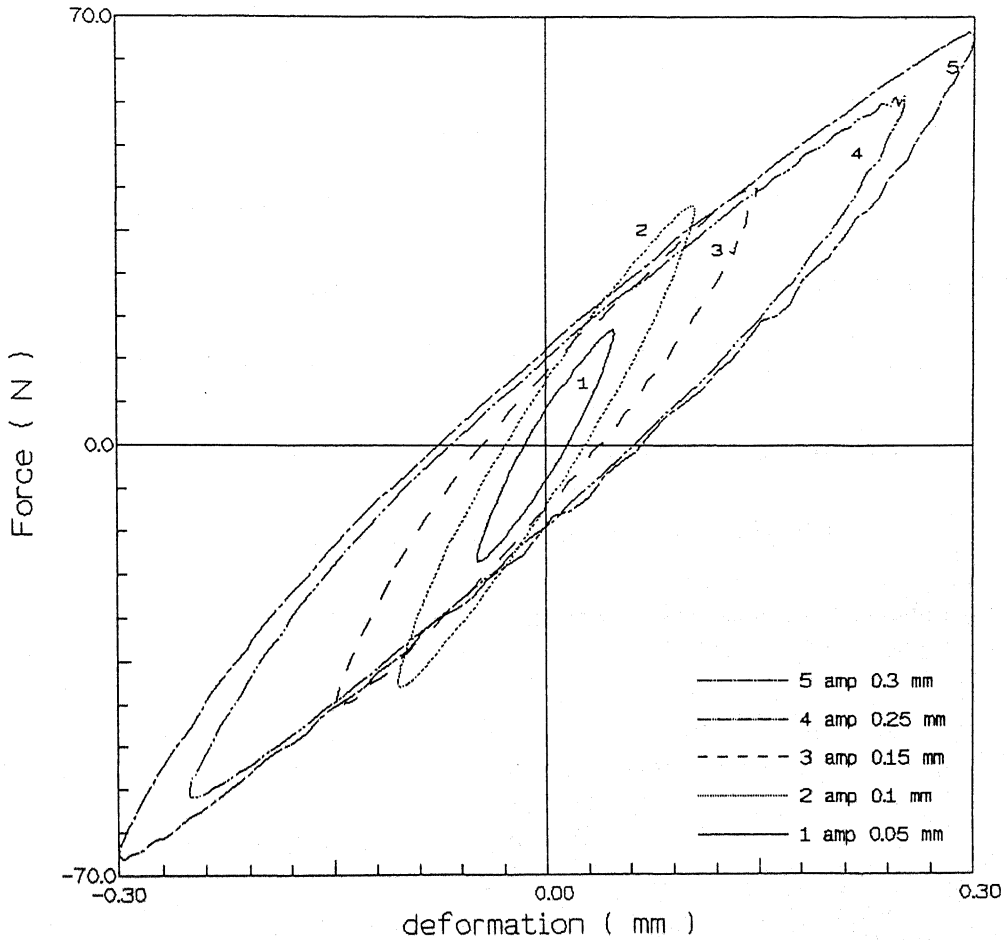

Figure 4.8: Hysteresis loops (0.05 mm, 0.1 mm, 0.15 mm, 0.25 mm, 0.3 mm deformation amplitude; 60 Hz)

nearly elliptical. The fact that the shape of the hysteresis loop does not undergo any noticeable change also indicates that the form of the damping force remains same with changing amplitude and frequency.

4.5 Proposed Model

The main objective of the present work is to frame the constitutive equation for the rubber spring which gives an idea about the stiffness properties of the rubber isolator and exact damping mechanisms responsible for its dynamic behaviour.

In order to formulate a model for the rubber spring, the observations from figures 4.1 to 4.8 (discussed in earlier sections) are reproduced briefly here.

Ob. 1 Static stiffness test (Fig. 4.1) indicates a softening type spring.

Ob. 2 Dynamic stiffness is indipendent of the frequency (Fig. 4.3).

Ob. 3 Dynamic stiffness decreases with increasing deformation amplitude Z_0 (Fig. 4.8).

Ob. 4 The dynamic stiffness is linear with the deformation z at a particular deformation amplitude Z_0 (Figures 4.3 and 4.8).

Ob. 5 The damping energy index is less than 2 (Figures 4.6 and 4.7).

Ob. 6 The damping energy is independent of the frequency (Figures 4.4 and 4.5) in the range of frequency normally encountered in the structural vibrations.

Ob. 7 The contribution of different damping mechanisms is independent of frequency and the deformation amplitude (Fig. 4.8).

The observations (1) and (3) rule out the possibility of using stiffness from the static test because $F_s(z)$, modelled with the static stiffness, cannot take care of

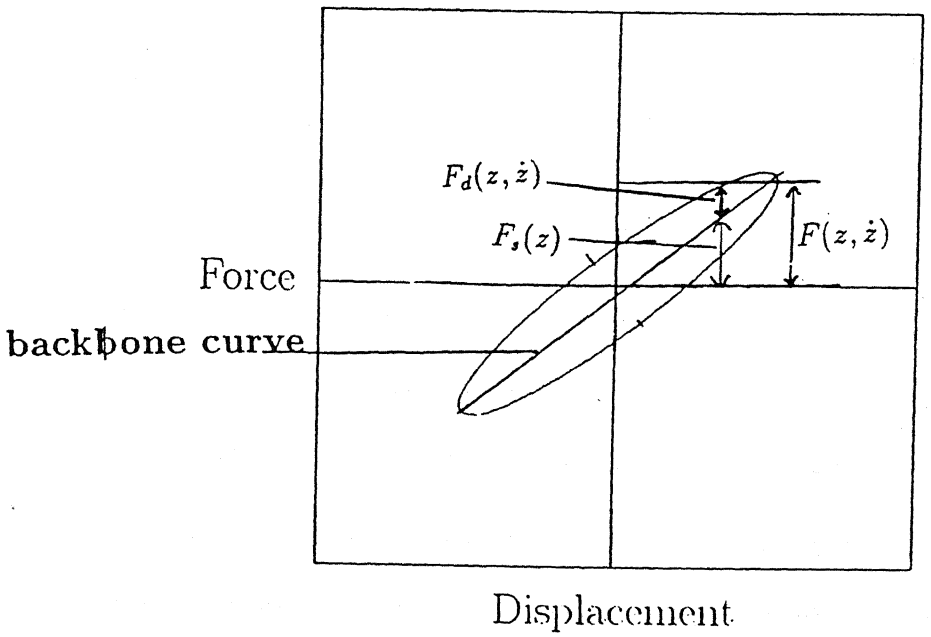

Figure 4.9: Components of $F(z,\dot{z})$

the rotation of the loops with increasing amplitudes. It is worthwhile to recall here that the model $F(z,\dot{z})$ (eqn. 2.3) consists of $F_s(z)$ and $F_d(z,\dot{z})$, as is illustrated in Fig. 4.9. It is apparent that only the term $F_s(z)$ can account for observation (3). Now observation (4) suggests a model $F_s(z) = K_{dyn}z$ where K_{dyn} should show dependence upon deformation amplitude Z_0 (Observation (3)). Therefore, K_{dyn} was selected as $K_{dyn} = a - b|Z_0|^q$ where a, b and q will be determined through least square fit.

The damping model $F_d(z,\dot{z})$ is taken to be consisting of two parts, one part representing hysteretic damping and the other part representing Coulomb damping, because of the following reasons. The elliptical shape of the hysteresis loops along with the observation (6) directly indicates the presence of hysteretic damping. However, the observation (5) indicates that in conjunction with the hysteretic

damping (for which $p = 2$), there should be another damping term having the specific damping energy exponent p less than 2. Since Coulomb damping yields the damping energy exponent $p = 1$, the damping model is taken to be a combination of hysteretic and Coulomb damping such that

$$F_d(z, \dot{z}) = f_{col}\, sgn(\dot{z}) + \left(\frac{h}{\omega}\right) \dot{z} \tag{4.1}$$

However, the above model needs another refinement because eqn 4.1 will result in a hysteresis loop with sharp corners in contrast to the hysteresis loops observed in Fig. 4.8. The sharp corners result because of jump in f_{col} at $\dot{z} = 0$.

This is noteworthy that the dry friction $f_{col}\, sgn(\dot{z})$ being independent of the magnitude of the velocity is the idealization of the actual Coulomb friction behaviour [14, 15]. Due to different contributions of the molecular friction and effects of the fillers in the rubber, the form of the Coulomb friction may vary with frequency and amplitude, and this is distinctly different from the structural materials [16]. In the proposed model too, the Coulomb friction is modelled as increasing with velocity wihtin a small velocity zone starting from zero at zero velocity and dropping to a constant value with further increase in the velocity. This kind of behaviour of the dry friction has been reported in reference [17] where the dry friction characteristics of polymeric seals have been discussed. Therefore, F_d is finally expressed as

$$F_d = \left(\frac{h}{\omega}\right) \dot{z} + \left[f_{col} + C_1 e^{-C_2|(|\dot{z}|-C_3)|} - \left(f_{col} + C_1 e^{-C_2 C_3}\right) e^{-C_4|\dot{z}|}\right] sgn(\dot{z}) \tag{4.2}$$

The behaviour of the Coulomb friction in this model is shown in Fig. 4.10. In order to confirm to the observations (5) and (6) of the damping energy behaviour, f_{col} and h in the above term should not be much different from those in equation

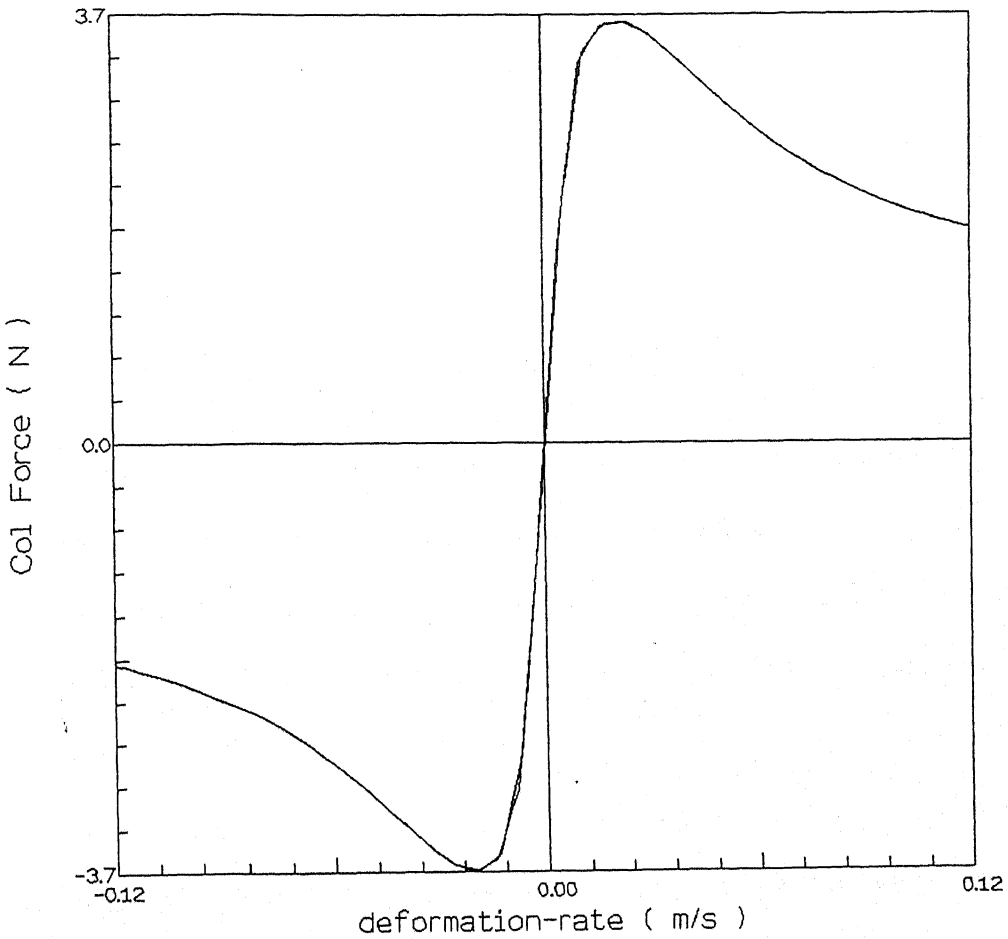

Figure 4.10: Variable Coulomb friction force employed in the model)

4.1. Also C_1, C_2, C_3 and C_4 are so selected (through trial and error) that these constants do not affect the energy dissipation over a cycle but at the same time, do contribute in rounding the corners in hysteresis loops. With the above observation, the energy dissipation per cycle can be written as

$$E_{damp} = \pi h|Z_0|^2 + 4f_{col}|Z_0| \tag{4.3}$$

The constitutive equation of the system is expressed as

$$m\ddot{x}+\left(\frac{h}{\omega}\right)\dot{z}+\left[f_{col} + C_1 e^{-C_2|(|\dot{z}|-C_3)|} - \left(f_{col} + C_1 e^{-C_2 C_3}\right) e^{-C_4|\dot{z}|}\right] sgn(\dot{z})+K_{dyn}z = 0 \tag{4.4}$$

where

$$K_{dyn} = a - b|Z_0|^q \tag{4.5}$$

m, the mass of the plate and the steel block on the rubber spring including the mass of the accelerometer, was measured to be 2.2 Kg. For constants a, b, q in equation 4.5, the dynamic stiffness K_{dyn} at 60 Hz for different deformation amplitudes $|Z_0|$ was calculated (Fig. 4.8). Thereafter, the method of least squares was used for finding out a, b, q in equation 4.5.

From equation 4.3, the damping energy E_{damp} of the model (equation 4.4) is given as $\pi h|Z_0|^2 + 4f_{col}|Z_0|$. The constants h and f_{col} were determined from the damping energy variation with deformation amplitude $|Z_0|$ at 60 Hz (Fig. 4.6) by least square fit. The damping energy index in Fig. 4.6 is 1.5 and that obtained by calculated values of h and f_{col} is 1.48.

Constants C_1, C_2, C_3, C_4 were calculated by trial and error. It is observed that C_3 gives the value of the velocity around which the Coulomb friction term attains the maximum value and this should be small so as to lie near zero. Though both

C_2 and C_4 influence the variation of friction with velocity, yet, C_2 dominates the behaviour of the friction force after attaining the maximum value and C_4 affects its increase from zero to the maximum value. The values of the above constants are tabulated in the table 4.1.

Since this model involves K_{dyn} which is a function of the deformation amplitude $|Z_0|$, it has to be solved by trial and error. The experimental and simulated loops are shown in Figures 4.11 to 4.14.

Table 4.1: Values of the constants in the constitutive equation

Constant name	Symbol	Unit	Value
mass	m	Kg	2.2
hesteretic damping Co-efficient	h	Kg/s^2	2.11×10^{-3}
Coulomb friction Co-efficient	f_{col}	N	1.5
	C_1	N	3.5
	C_2	$m^{-1}s$	20.0
	C_3	ms^{-1}	0.01
	C_4	$m^{-1}s$	90.0
	a	N/m	1476917.4
	b	$N/m^{1.1}$	2839317.7
	q		0.1

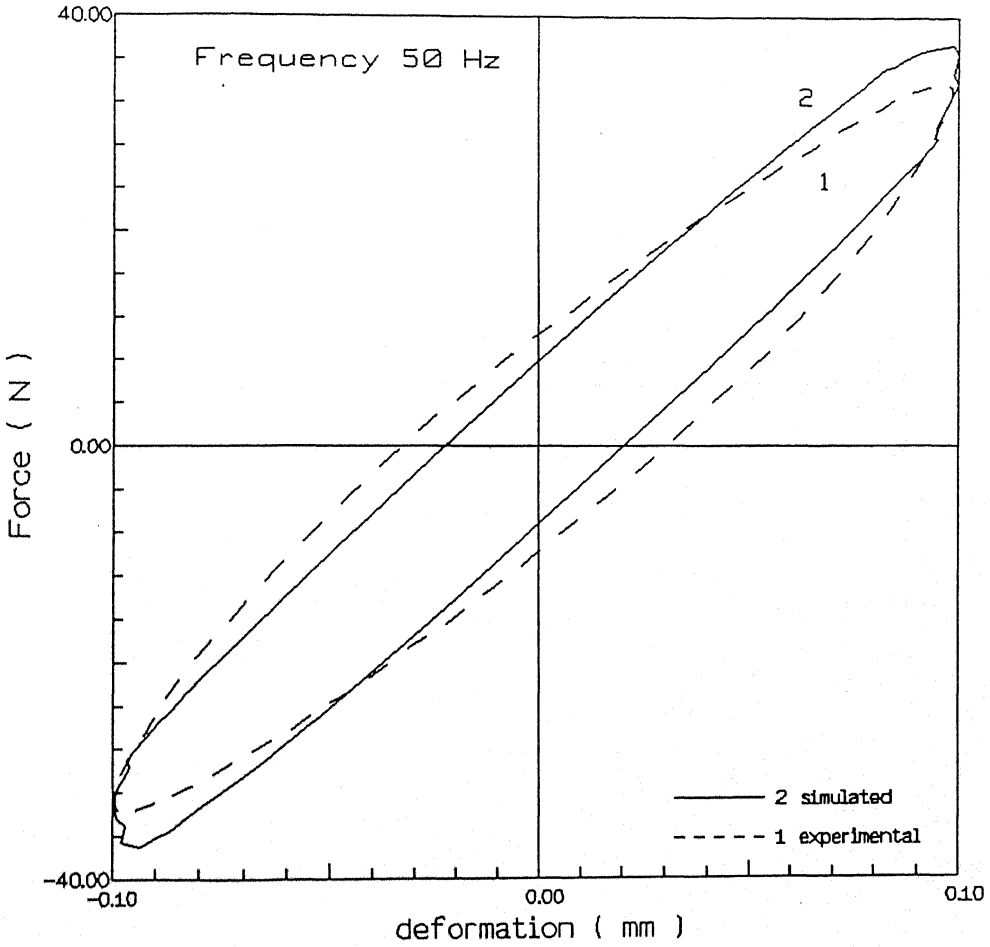

Figure 4.11: Experimental and simulated hysteresis loops (50 Hz, 0.1 mm deformation amplitude)

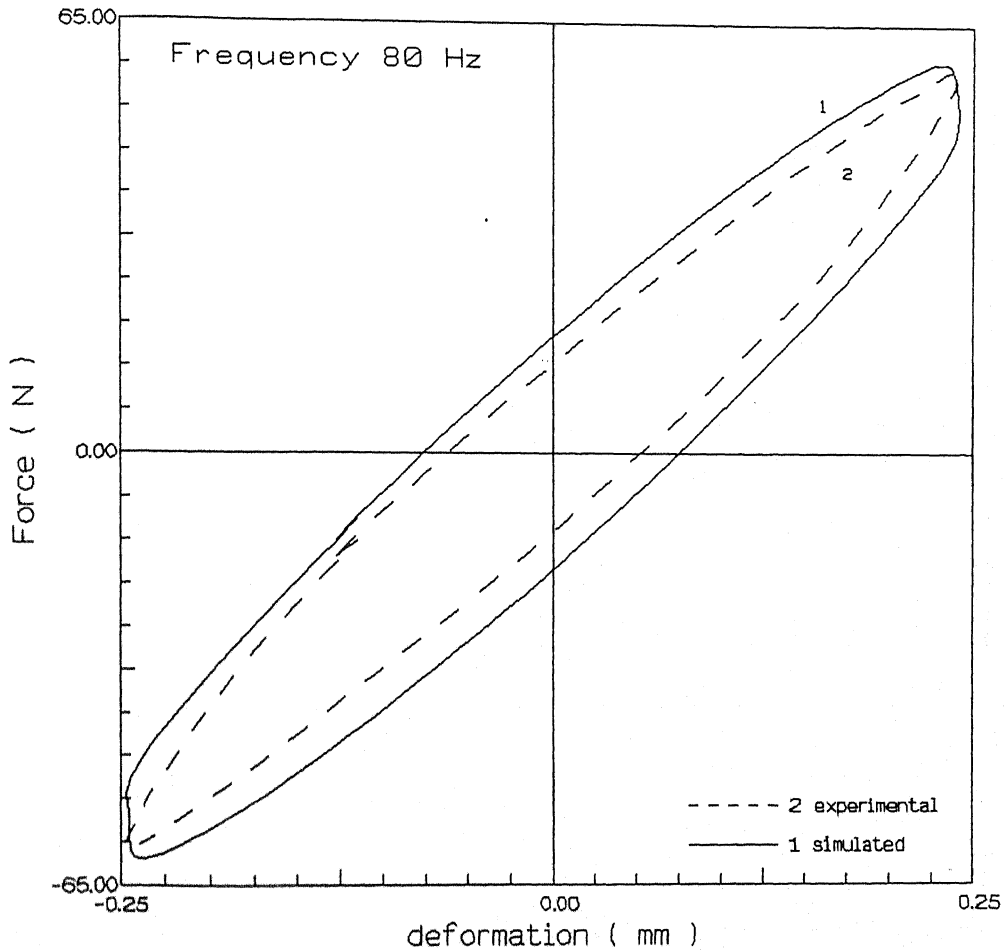

Figure 4.12: Experimental and simulated hysteresis loops (80 Hz, 0.25 mm deformation amplitude)

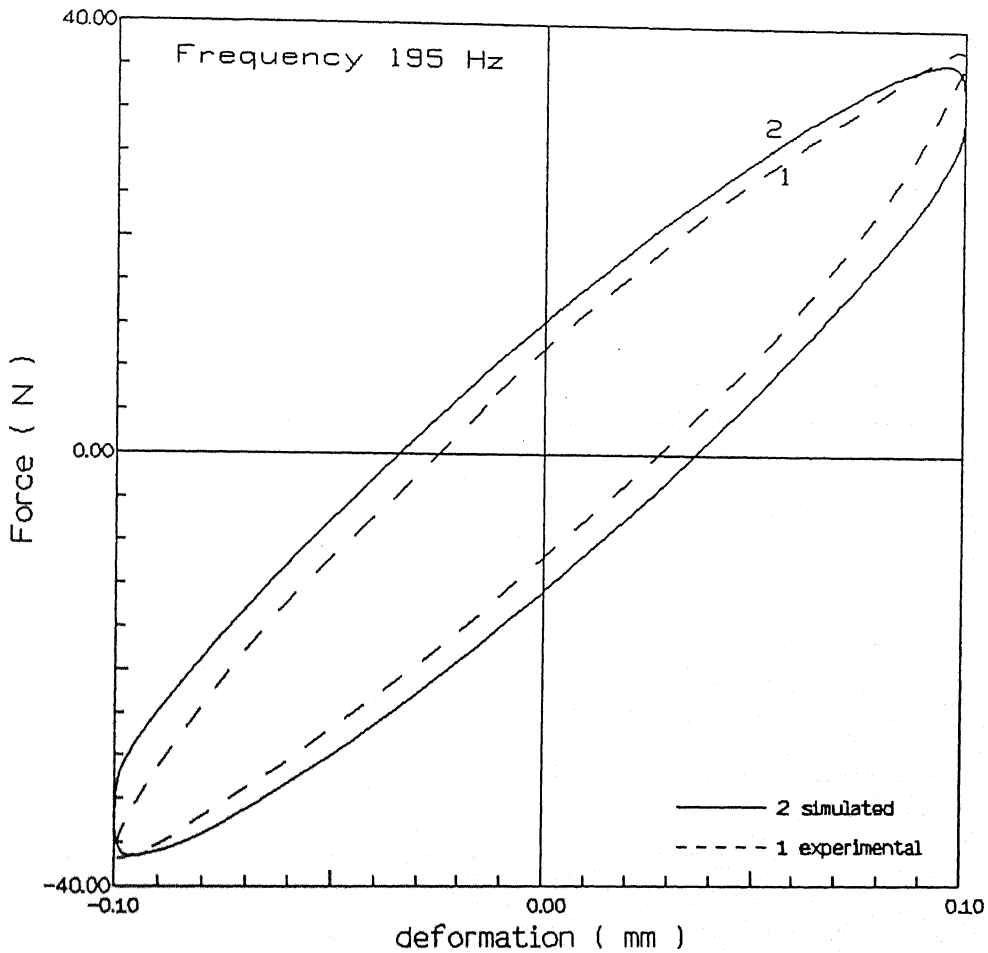

Figure 4.13: Experimental and simulated hysteresis loops (195 Hz, 0.1 mm deformation amplitude)

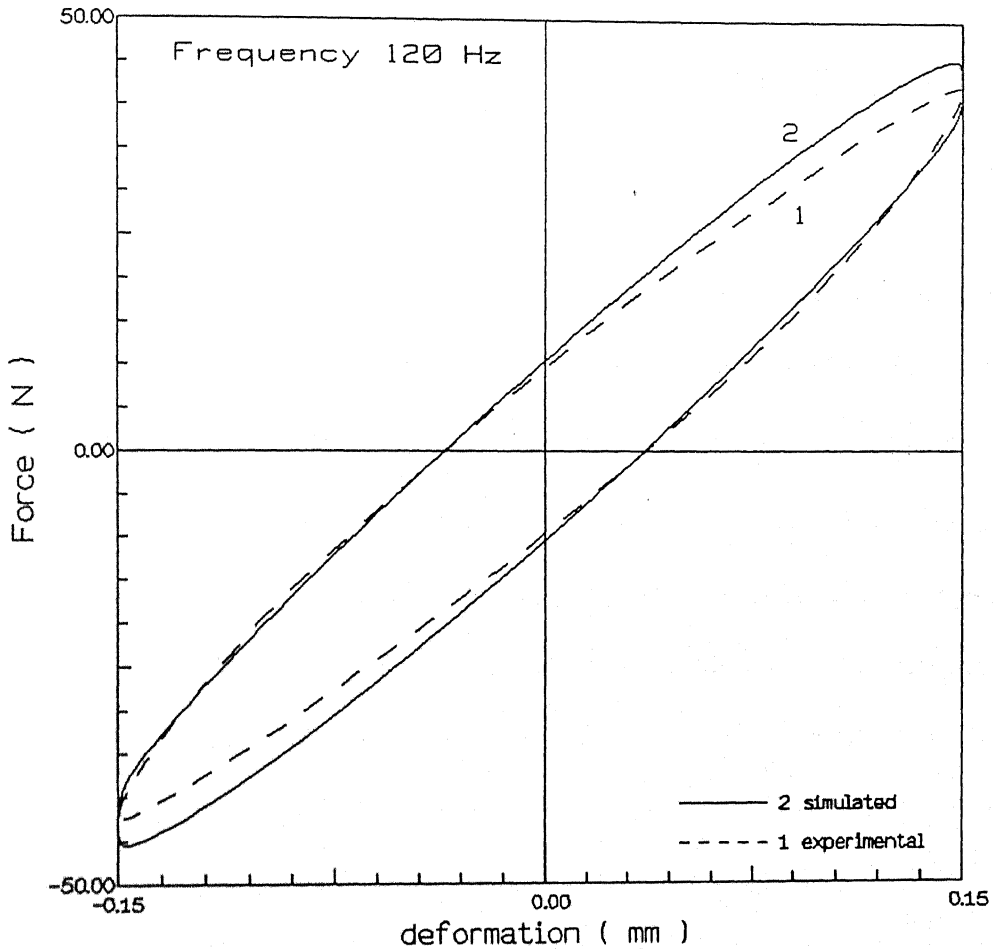

Figure 4.14: Experimental and simulated hysteresis loops (120 Hz, 0.15 mm deformation amplitude)

Chapter 5

Conclusions

The dynamic characteristics of a rubber spring under harmonic loading have been studied. The shape of the hysteresis loops and the variation of the damping energy with deformation of the rubber spring leads to the following conclusions.

[i] Both linear hysteresis damping and non-linear Coulomb damping, need to be combined for representing the damping force. The hysteresis damping was adopted in the model, since the energy dissipated per cycle failed to show any characteristic variation with the frequency. Of course, the variation of damping energy with frequency showed considerable amount of scatter.

[ii] The backbone curves of the hysteresis loops, while remaining straight, changed orientation at different amplitudes. This behaviour has also been reported in earlier works. Consequently, this amplitudes dependence of the dynamic stiffness needs to be modelled properly.

[iii] A constitutive equation, under harmonic loading, has been proposed and seen to fit the results at room temperature within the limited range of frequency.

5.1 Scope of future work

The proposed experimental method should be rigorously tested in a wider range of frequency and a large number of samples which could not be done due time constrant. The effects of temperature on the dynamic characteristics of rubber, known to be important, should be studied. Various configurations of standard metal-bonded rubber springs can be tested and proper models prepared for each configurations.

References

[1] Weissman P. T. and Richard P. Chartoff, Extrapolating Visco-elastic Data in the Temperature–Frequency Domain. *In* Corsaro R. D. and Sperling L. H. (ed.), *Sound and Vibration Damping with Polymers*, American Chemical Society 1990.

[2] Ferry J. D., *Visco-elastic properties of polymers*, Chapter 11, John Willy and Sons, Inc. 1980.

[3] Kerwin E. M., Jr. and Unger E. E., Requirements Imposed on Polymeric materials by Structural Damping Applications, *In* Corsaro R. D. and Sperling L. H. (ed.), *Sound and Vibration Damping with Polymers*, American Chemical Society 1990.

[4] Draker M. L., General Approach to Damping Design, *In* Corsaro R. D. and Sperling L. H. (ed.), *Sound and Vibration Damping with Polymers*, American Chemical Society 1990.

[5] Tinker M. L. and Cutchins M. A., Damping Phenomenon in a Wire Rope Vibration Isolation System, *Journal of Sound and Vibraton* (1992) Vol. **157**(1), pg. 7–18.

[6] Harris J. and Stevensen A., On the Role of Non-linearity in the Dynamic Behaviour of Rubber Components, *Rubber Chemistry and Technology* Vol. 59,

No. 5, pg. 740–764, 1986.

[7] Harris J., Dynamic Testing under Non-sinusoidal Conditions and the Consequences of Non-linearity on Service Performance, *Rubber Chemistry and Technology*, Vol. 60, No. 5, pg. 870–887, 1987.

[8] Medalia A. J., Effect of Carbon Black on Dynamic Properties of Rubber Vulcazinates, *Rubber Chemistry and Technology*, Vol. 51, No. 3, pg. 437–523, 1987.

[9] Nakajima N. and Collins E. A., Viscoelastic Properties of SBR containg Particles of Cross-linked Polysterene, *Rubber Chemistry and Technology*, Vol. 51, No. 1, pg. 110–116, 1978.

[10] Vinogradov O. and Pivovarov I., Vibration of A System with Non-linear hysteresis, *Journal of Sound and Vibration*, Vol. 111, No. 1, pg. 145–152, 1986.

[11] Iyenger R. N., Inelastic Response of beams under Sinusoidal and Random Loads, *Journal of Sound and Vibration*, Vol. 64, No. 2, pg. 161–172, 1979.

[12] Lazan B. J., *Damping of Materials and Members in Structural Mechanics*, Pergamon Press Inc., 1968.

[13] Göbel E. F., *Rubber Springs Design*, Newnes-Butterworths, London 1974.

[14] Jorden O. W. and Smith P., *Non-linear Ordinery Differential Equations*, (2nd ed.)Oxford University Press, Oxford, 1987.

[15] Roberts J. B. and Spanos P. D., *Random Vibration and Statistical Linearization*, John Willey and Sons, Chichester, 1990.

[16] Payne A. R., The Role of Hysteresis in Polymers, *Rubber Journal*, Vol. 146, 80th year, No. 1, 1964.

[17] Nau B. S., The State of the Art Rubber Seal Technology, *Rubber Chemistry and Technology*, Vol. 60, No. 3, pg. 381–416, 1987.

Appendix

1. I. M. V. electrodynamic shaker

Max. force output	:	80 Kgf (wihout load)
Max. acceleration	:	47g
Max. velocity	:	41 cm/sec
Max. displacement	:	25 mm pp
Weight of the moving element	:	1.7 kg
Frequency range	:	5–5000 Hz
Max. loading weihgt	:	70 Kg
Rating	:	24 Hours continuous duty (ambient temperature 0–40° C)
Power consumption	:	3.5 KVA

2. Accelerometers

Make	:	B & K, Type 4370
Reference sensitivity	:	at 159.2 Hz, 100 ms^{-2} and 23° C
Charge sensitivity	:	10.20 pc/ms^{-2}
Capacitance (including cable)	:	1188 pF
Frequency range	:	upto 25 kHz

3. Oscilloscope

Make	:	Kikusui COR 5501U
Input impedence	:	1 mega-ohm ± 2 %, 21 pF ± 2 pF
Max. allowable input voltage	:	400 V peak (DC + AC peak)
Channel section	:	CH1, ADD (CH1 ± CH2)
		CH2, CH2 INV, DUAL (CHOP,ALT)
Time difference among two channels	:	± 500 ps or less
Sweep speed (time base)	:	Real 20 ns/DIV – 0.5 s/DIV
		Storage 20 ns/DIV – 5 s/DIV
X–Y phase shift	:	DC–100 kHz within 3 degrees

4. Charge amplifier

Make	:	B & K 2635
Charge input	:	10^5 pC max. input rating
Transducer sensitivity conditioning	:	3 digit dial in of transducer
		sensitivity from 0.1 to 0.99 pc/ms^{-2}
Amplifier sensitivity	:	0.1 mV to 10 V/pC
		corresponding to -40 to +80 dB
		with transducer capacitance of 1 nF
Calibrated output ratings	:	selectable in 10 dB steps
		Acceleration — o.1 mV to 1 V/ms^{-2}
		Velocity — 10 mV to 100 V/ms^{-1}
		Displacement — o.1 mV to 10 V/mm
Maximum output	:	8 V (8 mA) peak
output impendence	:	< 1 ohm

122010

Date Slip

This book is to be returned on the date last stamped.

122010

ME-1995-M-KHE-MOD

A122010